Available online at www.sciencedirect.com
ScienceDirect
Catalysis Today 125 (2007) 239–247
CATALYSIS TODAY
www.elsevier.com/locate/cattod

Effect of phosphorus addition on the hydrotreating activity of $NiMo/Al_2O_3$ carbide catalyst

V. Sundaramurthy [a], A.K. Dalai [a,*], J. Adjaye [b]

[a] *Catalysis and Chemical Reaction Engineering Laboratories, Department of Chemical Engineering, University of Saskatchewan, Saskatoon, SK S7N 5A9, Canada*
[b] *Syncrude Edmonton Research Centre, Edmonton, AB T6N 1H4, Canada*

Abstract

A series of phosphorus promoted γ-Al_2O_3 supported NiMo carbide catalysts with 0–4.5 wt.% P, 13 wt.% Mo and 2.5 wt.% Ni were synthesized and characterized by elemental analysis, pulsed CO chemisorption, BET surface area measurement, X-ray diffraction, near-edge X-ray absorption fine structure, DRIFT spectroscopy of CO adsorption and H_2 temperature programmed reduction. X-ray diffraction patterns and CO uptake showed the P addition to NiMo/γ-Al_2O_3 carbide, increased the dispersion of β-Mo_2C particles. DRIFT spectra of adsorbed CO revealed that P addition to NiMo/γ-Al_2O_3 carbide catalyst not only increases the dispersion of Ni-Mo carbide phase, but also changes the nature of surface active sites. The hydrodenitrogenation (HDN) and hydrodesulfurization (HDS) activities of these P promoted NiMo/γ-Al_2O_3 carbide catalysts were performed in trickle bed reactor using light gas oil (LGO) derived from Athabasca bitumen and model feed containing quinoline and dibenzothiophene at industrial conditions. The P added NiMo/γ-Al_2O_3 carbide catalysts showed enhanced HDN activity compared to the NiMo/γ-Al_2O_3 catalysts with both the feed stocks. The P had almost no influence on the HDS activity of NiMo/γ-Al_2O_3 carbide with LGO and dibenzothiophene. P addition to NiMo/γ-Al_2O_3 carbide accelerated C–N bond breaking and thus increased the HDN activity.

Keywords: P promoted NiMo/γ-Al_2O_3 carbide; DRIFT of CO adsorption; Hydrodesulfurization; Hydrodenitrogenation; Light gas oil; Quinoline; Dibenzothiophene

1. Introduction

Demands for a cleaner environment have led to a global tightening in the allowed sulfur content in transportation fuels. Because of the recent and future legislations concerning air pollution by exhaust gases from diesel engines, new types of hydrotreating catalysts, which are economic, have long-life, and possess higher activity than the conventional sulfide catalysts are highly desired. It has been well demonstrated that unsupported and supported Mo_2C have excellent potential for use in hydrodenitrogenation (HDN) and hydrodesulfurization (HDS) reactions [1–17]. The majority of these studies have found that bulk and supported Mo carbide catalysts to have HDN and HDS activities similar to or higher than those of corresponding conventional sulfide catalysts.

Additives such as P have a promotional effect when added to the oxide forms of the catalyst. In the past two decades, phosphorus has been especially incorporated into *in situ* sulfided NiMo/γ-Al_2O_3 bimetallic catalyst. Most of the reports showed that P addition to NiMo/γ-Al_2O_3 sulfide catalysts promote both HDN and HDS [18–21]. But a few studies [19,22] showed that phosphorus addition to NiMo/γ-Al_2O_3 sulfide catalysts did not affect the HDS activity, whereas it promoted the HDN. These effects are typically explained in terms of dispersion of the metal salts on the support, modification of acid sites or formation of a new active phase.

Phosphorus acts as a promoter in monometallic molybdenum carbides [12,14,23,24] for HDN and HDS reactions as it does in the monometallic molybdenum sulfides. Mostly, the promotional effect of phosphorus in metal carbides has been explored using model compounds such as dibenzothiophene [14], quinoline [14] and tetralin hydrogenation [24]. No report is available on hydroprocesing of real feeds using supported

---

* Corresponding author. Tel.: +1 306 966 4771; fax: +1 306 966 4777.
E-mail address: ajay.dalai@usask.ca (A.K. Dalai).

0920-5861/$ – see front matter © 2007 Elsevier B.V. All rights reserved.
doi:10.1016/j.cattod.2007.01.056

bimetallic carbides containing phosphorus, especially γ-Al_2O_3 supported NiMo carbides.

There has been some work on P containing NiMo carbides and nitrides and their HDS activity in thiophene and dibenzothiophene [25]. However, information available on the effect of P in NiMo carbide catalysts and their reactivity for HDS is very limited [25]. Further, the detailed study on HDN promotional effect of P in γ-Al_2O_3 supported NiMo carbide is scarce in literature. In the current investigation, a series of γ-Al_2O_3 supported nickel molybdenum bimetallic carbide catalysts containing various amounts of phosphorus were synthesized by temperature programmed reaction (TPR) using a bimetallic oxide as the precursor. The effect of P on the NiMo/γ-Al_2O_3 carbide structure and their HDN and HDS activities with light gas oil derived from Athabasca bitumen and a model feed containing quinoline and benzothiophene were studied under industrial conditions.

2. Experimental

2.1. Catalyst preparation

The preparation of the carbide catalysts was carried out in two stages. The first stage involved the preparation of oxide precursors of desired composition by an incipient wetness co-impregnation method. In the second stage, oxide precursors were converted into carbides by TPR. The support, extruded γ-alumina of 1 mm diameter and 8 mm length (Sud Chemie, India) was calcined at 500 °C (ramp rate of 3 °C/min) for 3 h prior to impregnation. A series of P doped $NiO{\cdot}MoO_3/Al_2O_3$ precursors (13 wt.% Mo and 2.5 wt.% Ni) with various amount of P (0–4.5 wt.%) were prepared by impregnation of γ-Al_2O_3 with aqueous solution (pH ~ 4) containing the appropriate amounts of ammonium heptamolybdate (99.9%, Aldrich), nickel nitrate (99%, BDH) and phosphoric acid (AnalaR, BDH). The impregnated samples were dried at 120 °C for 5 h and then calcined at 500 °C for 5 h in air. Carbides were prepared by TPR of the oxide precursors in flowing 20% CH_4/H_2 (v/v). A typical synthesis consists of loading about 10 ml of the oxide precursor in an inconel reactor placed in a tubular furnace (Applied Test Systems, Inc. series 3210) controlled by a temperature programmer (Eurotherm 2416). First the sample was heated to 400 °C at rate of 3 °C/min in flowing He (flow rate 50 cm^3/min). At this temperature, the flow was switched to 20% CH_4/H_2 (v/v) gas mixture at a flow rate of 50 cm^3/min and then the temperature was ramped at 1 °C/min from 400 to 700 °C. The carburization of sample was monitored by analyzing the consumption of methane and the formation of CO and CO_2 by using gas chromatography (HP 5890 series II). The 20% CH_4/H_2 (v/v) gas mixture passed through the sample until no carbon oxides were detected in the exhausted gas. Then the gas flow was switched from CH_4/H_2 to He, and the sample was quenched to room temperature. After cooling, the He gas was switched to a gas mixture containing 5% O_2 in He (v/v) for passivation. The carbide catalyst was passivated for 10 h to avoid a strong bulk oxidation. The prepared carbide catalysts are in the form of extrudates of 1 mm diameter and 8 mm length.

2.2. Characterization techniques

The contents of Ni, Mo and P in carbide catalyst were determined by plasma atomic emission method (ICP). Carbon content of carbide catalysts were carried out using CHNSO analyzer (Elementar Americas, Inc.) Surface area and pore volume were measured by means of the adsorption of N_2 at 78 K. Prior to the analysis, the samples were degassed in vacuum at 200 °C until the static pressure remained less than 6.6×10^{-4} Pa prior to analysis. Specific area was determined by the BET method. Powder X-ray diffraction (XRD) patterns of the catalysts were recorded on a Bruker diffractometer using Cu Kα radiation. The CO uptake on the catalysts was measured using the Micromeritics ASAP 2000 instrument. Before chemisorption measurement, 200 mg of sample was reduced with H_2 at 400 °C, and then evacuated until the static pressure remained less than 6.6×10^{-4} Pa. Pulses of CO were passed over the sample to measure the total gas uptake at 35 °C. Near-edge X-ray absorption fine structure (NEXAFS) measurement of carbide catalysts was carried out at the SGM beamline of the Canadian Light Source at University of Saskatchewan. The NEXAFS spectra were recorded near the K-edge of C by measuring the fluorescence electron yield.

Diffuse reflectance infrared Fourier transform spectroscopy (DRIFTS) of CO adsorption experiments were performed using a Perkin-Elmer Spectrum GX instrument equipped with DTGS detector and a KBr beam splitter. Approximately 30 mg of catalyst was loaded into a sample cup inside a Spectrotech diffuse reflectance *in situ* cell equipped with ZnSe windows and a thermocouple mount that allowed direct measurement of the sample surface temperature. Spectra for each experiment were averaged over 64 scans in the region 4000–1000 cm^{-1} with a nominal 4 cm^{-1} resolution. Prior to the CO adsorption, the carbide catalyst was activated in a Spectrotech diffuse reflectance *in situ* cell with H_2 at 400 °C for 2 h in order to remove the passivation oxide layer. At this temperature, the flow was switched to He at a flow rate of 50 cm^3/min and the temperature was decreased to 30 °C and then background spectrum was recorded. The adsorption process was carried out at 30 °C by introducing CO into the system for 30 min. After adsorption, the system was subsequently purged with He at a flow rate of 50 cm^3/min for 60 min. Then the spectra were collected under He flow and the background spectrum was subtracted from the post adsorption spectra. Band intensities were corrected for slight differences in the weight of the catalyst and normalized to 30 mg.

DRIFT of adsorbed CO measurements on sulfided carbide catalysts were carried out following the experimental procedure described above for the carbide catalysts, following *in situ* sulfidation prior to CO adsorption. The catalyst was activated in a Spectrotech diffuse reflectance *in situ* cell with H_2 at 400 °C for 2 h and then *in situ* sulfided with 10% H_2S/H_2 (50 cm^3/min) at 370 °C. For spent catalysts, prior to the CO adsorption, the catalysts were flushed with He (50 cm^3/min) at 200 °C for 1 h.

H_2-temperature programmed reduction (H_2-TPR) of the samples was carried out using a ChemBET-3000 instrument. A

200 mg sample in a quartz tube was purged with He at 400 °C for 1 h in order to remove impurities on the surface of the sample. After the sample was cooled to room temperature in flowing He, TPR was carried out in 3% H_2/N_2 (v/v) mixture with a flowing rate of 30 cm^3/min. The heating rate was 10 °C/min from room temperature to 600 °C. TPR profiles were recorded with a thermal conductivity detector.

2.3. Hydrotreating tests

The hydrotreating tests were carried out under steady-state operation in a trickle bed reactor in down-flow mode. The high pressure reaction set up used in this study simulates the process that takes place in an industrial hydrotreater. The system consists of liquid and gas feed sections, a high-pressure reactor, a heater with temperature controller for precisely controlling the temperature of the catalyst bed, a scrubber for removing the ammonium sulfide from the reaction products, and a high pressure gas–liquid separator. The reactor is made of a inconel tube; the length and internal diameter of the reactor are 240 and 14 mm, respectively. The detail of catalyst loading into the reactor is described elsewhere [26]. The reactor is divided into three sections. The first section was packed with silicon carbide and was used to heat up the mixture to the desired reaction temperature. The second section contained 5 cm^3 of catalyst (3.8 g) and 12 cm^3 of 90 mesh silicon carbide and the final section was also packed with silicon carbide. The model feed containing 2400 ppm of N and 6500 ppm of S is prepared by dissolving quinoline and benzothiophene in hexadecane solvent. The properties of the light gas oil used in the evaluations are given in Table 1.

Before each catalytic run, the passivated carbide catalyst was reduced in flowing H_2 at 400 °C for 2 h to remove passivation oxygen layer. Then, the catalyst was precoked with LGO at the rate of 5 cm^3/h for 5 days at temperature, pressure and H_2/feed ratio of 370 °C, 8.8 MPa and 600 (v/v), respectively, and then the catalytic activity was examined using LGO and model compounds at a constant reaction pressure of 8.8 MPa, H_2/feed ratio of 600 (v/v). The liquid hourly space velocity was maintained at 2 and 3 h^{-1} for LGO and model feed, respectively. The HDN and HDS activities were studied at 340, 350 and 360 °C with LGO, and then at 300 °C with model feed for 72 h at each temperature and products were collected at 24 h time interval. The products were stripped with N_2 for removing the dissolved NH_3 and H_2S. The product samples collected on the second and third days were used for the N and S analyses. The total nitrogen and sulfur content of the liquid product were measured by combustion/chemiluminence (ASTM D4629), and combustion/fluorescence (ASTM 5463) techniques, respectively in an Antek 9000 NS analyzer. The instrumental error in N and S analysis was 3%. The conversion is defined as follows: N conversion = $[(N_I - N_F)/N_I] \times 100$; S conversion = $[(S_I - S_F)/S_I] \times 100$, where N_I and S_I are initial nitrogen and sulfur content (wt.%), respectively and N_F and S_F are final nitrogen and sulfur content (wt.%), respectively. The catalysts after reaction are referred to as spent catalysts. The characterization of spent catalysts was done after through washing with acetone.

Table 1
Characteristics of LGO derived from Athabasca bitumen

Characteristic	LGO
Nitrogen (wt.%)	0.025
Sulfur (wt.%)	1.595
Density (g/ml)	0.90
Simulated distillation	
IBP (°C)	171
FBP (°C)	461

Characteristic, boiling range (°C)	LGO, hydrocarbon (wt.%)
IBP–250	37.6
250–300	21.2
300–350	20.7
350–400	14.5
401–450	4.8
450–500	1.2
500–600	0
600–650	0

3. Result and discussion

P promoted NiMo/γ-Al_2O_3 carbide catalysts with 13 wt.% Mo, 2.5 wt.% Ni and P loading of 0, 0.5, 1.5, 2.5, 3.0 and 4.5 wt.% were prepared and denoted as PNiMo(x), where x is the target P loading in weight percentage.

3.1. The elemental compositions, BET and chemisorption measurements

The elemental compositions, BET surface area, pore volume and CO uptake of P promoted and unpromoted NiMo/γ-Al_2O_3 carbide catalysts are given in Table 2. Elemental chemical analysis of carbide catalysts indicates that the values of Mo, Ni and P content are all equal to or slightly below the corresponding targeted values of 13 wt.% Mo, 2.5 wt.% Ni and 0.5, 1.5, 2.5, 3.5 and 4.5 wt.% P. The BET surface area and average pore volume of prepared carbide catalysts are slightly lower than the γ-Al_2O_3 support, which is about 246 m^2/g and 0.73 cm^3/g, respectively. This apparently is due to pore blockage of alumina by the Ni, P and Mo species. As shown in Table 2, the Mo/C ratio of carbide catalysts is higher than the stoichiometric value of 2. Similar result was observed with supported carbide catalysts [12,14,24]. This higher Mo/C ratio indicates a strong interaction between support and molybdate [24]. The number of accessible surface metal atoms on carbide catalysts was titrated by using carbon monoxide as a molecular probe. As shown in Table 1, the CO uptakes of P added NiMo/γ-Al_2O_3 series increases rapidly with increase of P loading from 0 to 2.5 wt.% as a result of improved dispersion. Further increase of P loading, did not show significant increase in CO uptake and levels off for P contents above 2.5 wt.%. Thus maximum dispersion of carbide species is obtained for 2.5 wt.% P loading.

Table 2
Elemental compositions, BET surface area, pore volume and CO uptake of P promoted and unpromoted NiMo/γ-Al_2O_3 carbide catalysts

Catalyst	Mo (wt.%)	Ni (wt.%)	P (wt.%)	Mo/C	BET surface area (m^2/g)	Pore volume (cm^3/g)	CO uptake (μmol/g)
γ-Al_2O_3	–	–	–	–	243	0.73	–
PNiMo(0)[a]	12.83	2.42	–	3.21	199	0.59	52
PNiMo(0.5)	12.37	2.49	0.55	3.33	188	0.53	57
PNiMo(1.5)	12.75	2.43	1.53	3.18	193	0.55	82
PNiMo(2.5)	12.97	2.39	2.47	3.38	192	0.55	111
PNiMo(3.5)	12.91	2.42	3.46	3.46	194	0.56	116
PNiMo(4.5)	12.64	2.46	4.41	3.27	190	0.54	119

[a] Numbers in the parentheses represent target P wt.%.

3.2. XRD and NEXAFS of P promoted and unpromoted NiMo/γ-Al_2O_3 carbide

The XRD patterns of the unpromoted NiMo/γ-Al_2O_3 carbide catalyst, PNiMo(0) along with γ-Al_2O_3 support are shown in Fig. 1. Although, the diffraction pattern of NiMo/γ-Al_2O_3 carbide shows predominant peaks of the Al_2O_3, the presence of β-Mo_2C on the Al_2O_3 support is evident from the less intense peaks at 38.5° and 44.5°. All the P promoted NiMo/γ-Al_2O_3 carbide catalysts show only peaks of γ-Al_2O_3 support and no characteristic peaks of β-Mo_2C phase were detected. The XRD pattern of PNiMo(2.5) catalyst from PNiMo(*x*) series is shown in Fig. 1c as a typical case. The P addition to NiMo/γ-Al_2O_3 increased the dispersion of β-Mo_2C on γ-Al_2O_3 support as evidenced by CO uptake, hence, it is difficult to distinguish the β-Mo_2C phase from γ-Al_2O_3.

The nature of carbon atoms in the prepared carbide catalysts was investigated by NEXAFS technique. Fig. 2 shows the NEXAFS spectra of C K-edge of PNiMo(0), PNiMo(0.5), PNiMo(1.5), PNiMo(2.5), PNiMo(3.5) and PNiMo(4.5) catalysts. All the carbide catalysts have two sharp peaks at 286 and 289 eV, and a relatively broad peak at 294.8 eV. These peaks are assigned to carbidic carbon [2,27]. The peaks at 286 and 289 eV are due to the transitions of C 1s electrons to the p-d (t_2g) and p-d (eg) hybridized orbitals, respectively [2,14,27,13]. The broad peak at 294.8 eV is due to the transition of C 1s electrons to an unoccupied orbital that involves contributions from 2p and 3p orbitals of carbon and the d and s states of metals [2,14,27,13]. The presence of small amount of graphite nature of carbon in all the carbide catalysts is evident from the weak feature at 291.5 eV [13].

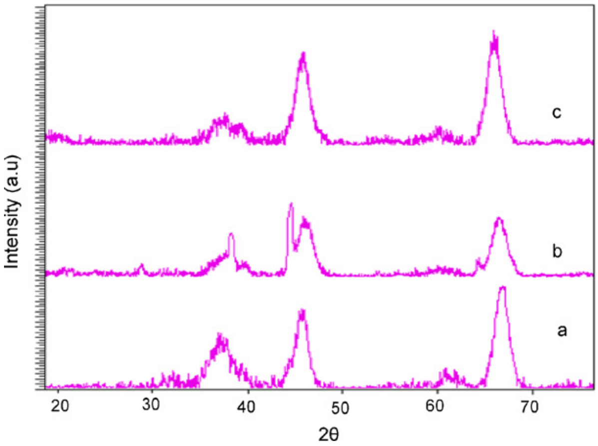

Fig. 1. XRD patterns of (a) γ-Al_2O_3, (b) PNiMo(0) and (c) PNiMo(2.5).

3.3. DRIFT spectroscopy of adsorbed CO on P promoted and unpromoted NiMo/γ-Al_2O_3 carbide catalyst

The surface sites on the carbide catalysts were characterized by DRIFT spectroscopy of adsorbed CO. DRIFT spectra of adsorbed CO on NiMo/γ-Al_2O_3 and P added NiMo/γ-Al_2O_3 carbide catalysts are given in Fig. 3. The NiMo/γ-Al_2O_3 carbide catalyst exhibits a strong band at 2000 cm^{-1} along with weak bands at 2030 and 2053 cm^{-1}, corresponding to Mo^0, Mo^{+1} and Mo^{+2} species, respectively [28–31]. As shown in Fig. 3, the P promoted NiMo/γ-Al_2O_3 carbide catalysts have quite different CO adsorption pattern from NiMo/γ-Al_2O_3 carbide catalyst. A new strong band at 2080 cm^{-1} corresponding to Mo^{3+} species [28–31] is formed on P addition to NiMo/γ-Al_2O_3 carbide catalysts. Further the band intensity at 2000 cm^{-1} decreased with P loading and disappeared when P loading exceeded 2.5 wt.%. Among the P added NiMo/γ-Al_2O_3 carbide catalysts, the intensity of bands at 2080, 2053 and 2030 cm^{-1} increased with P loading and reached optimum for 2.5 wt.% of P loading. The DRIFT of adsorbed CO study showed that P addition not

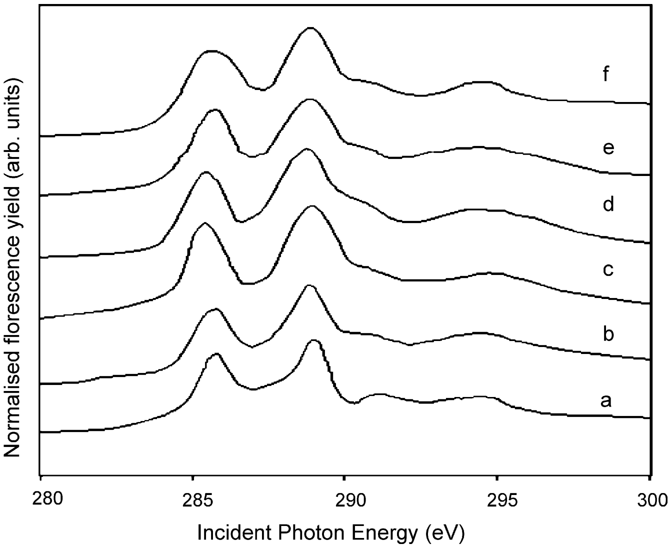

Fig. 2. C K-edge NEXAFS spectra of (a) NiMo(0), (b) PNiMo(0.5), (c) PNiMo(1.5), (d) PNiMo(2.5), (e) PNiMo(3.5) and (f) PNiMo(4.5) catalysts.

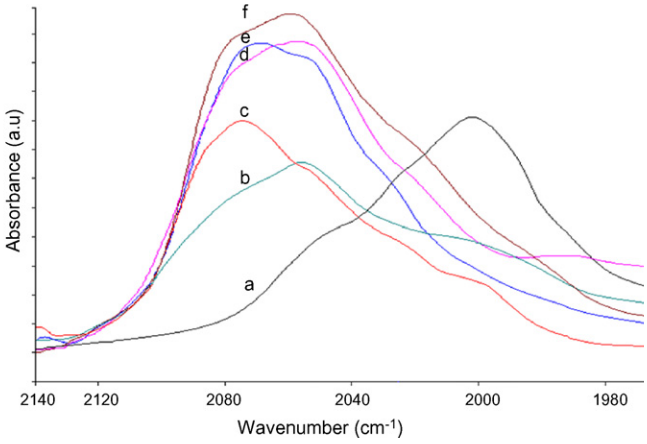

Fig. 3. DRIFT spectra of adsorbed CO on reduced passivated (a) PNiMo(0), (b) PNiMo(0.5), (c) PNiMo(1.5), (d) PNiMo(2.5), (e) PNiMo(3.5) and (f) PNiMo(4.5) catalysts.

only increased the number of accessible surface sites but also altered the nature of surface sites.

In order to get insight into the H_2S gas influences on the surface active sites of NiMo/γ-Al_2O_3 and P promoted NiMo/γ-Al_2O_3 carbide catalysts, representative catalysts such as PNiMo(0) and PNiMo(2.5) were treated with 10% H_2S/H_2 (v/v) gas mixture (50 cm^3/min) in the *in situ* DRIFT cell for 60 min at 370 °C and then the nature of the surface sites of catalysts was studied by DRIFT spectroscopy of adsorbed CO at 30 °C. Prior to the H_2S/H_2 treatment the passivated carbide catalysts were reduced at 400 °C. Fig. 4 presents the DRIFT spectra of CO adsorbed on PNiMo(0) and PNiMo(2.5) catalysts pretreated with a H_2S/H_2 gas mixture. The CO adsorption patterns of the H_2S/H_2 pretreated above catalysts are quite different from that of corresponding untreated carbide catalysts. A new band at 2094 cm^{-1} is observed with the H_2S/H_2 pretreated carbide catalysts. The band position of the CO absorbance, 2094 cm^{-1}, is similar to that of adsorbed CO on the sulfided Mo/Al_2O_3 catalyst which generally exhibits CO absorbance at around 2100 cm^{-1} [32–35]. The formation of the band at 2094 cm^{-1} indicated the partial sulfidation of the Mo carbide surface in the presence of H_2S/H_2 at 370 °C.

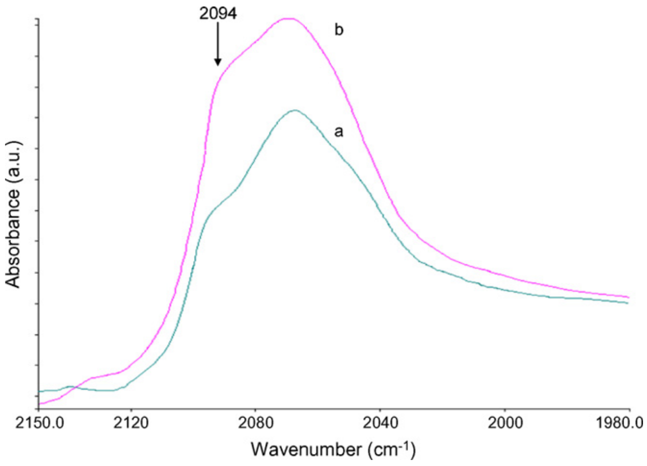

Fig. 4. DRIFT spectra of adsorbed CO on carbide catalysts pretreated with a 10 mol% H_2S/H_2 mixture at 370 °C (a) PNiMo(0) and (b) PNiMo(2.5).

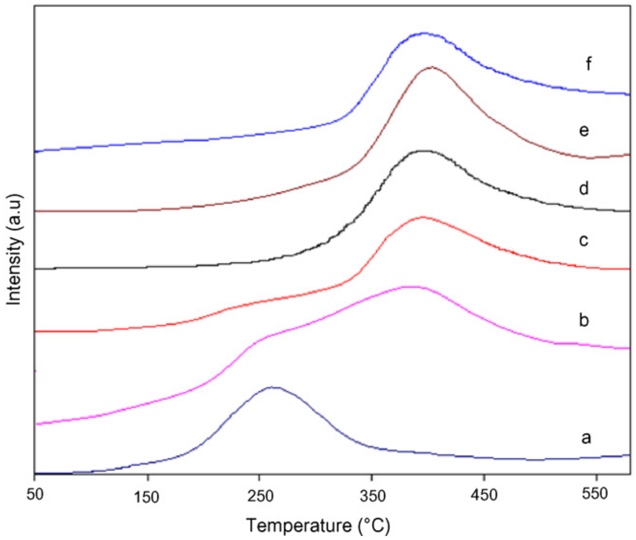

Fig. 5. H_2-TPR of passivated (a) PNiMo(0), (b) PNiMo(0.5), (c) PNiMo(1.5), (d) PNiMo(2.5), (e) PNiMo(3.5) and (f) PNiMo(4.5) carbide catalysts.

3.4. H_2-temperature programmed reduction

H_2-TPR profiles of the passivated carbide catalysts are shown in Fig. 5. The NiMo/γ-Al_2O_3 carbide catalyst exhibits a H_2 consumption peak at 255 °C. The P containing NiMo/γ-Al_2O_3 carbide catalysts have quite different TPR profiles than that of NiMo/Al_2O_3 carbide. The P promoted NiMo/γ-Al_2O_3 carbide catalysts showed major H_2 consumption peak at 360 °C along with shoulder at 255 °C. The intensity of peak at 255 °C is decreased with increase of P content from 0.5 to 1.5 wt.% and disappeared on further P addition. The peaks at 360 and 255 °C are due to reduction of surface oxygen bonded to Mo species of different states [36]. The gradual shift of 255–360 °C on P addition showed that nature of surface Mo species in NiMo/γ-Al_2O_3 carbide significantly changed with P content. This observation is in agreement with the result of DRIFT study of adsorbed CO on carbide catalysts.

3.5. Catalytic properties

3.5.1. Catalyst stabilization

To achieve steady state activity, the activated carbide catalysts were stabilized by precoking using LGO at the temperature, pressure, LHSV and H_2/feed ratio of 370 °C, 8.8 MPa, 2 h^{-1} and 600 ml/ml, respectively for 5 days. The catalyst stabilization curve of all the carbide catalysts in terms of N and S conversions, respectively are shown in Figs. 6 and 7, respectively. The N and S conversions of LGO over P promoted and unpromoted NiMo/Al_2O_3 carbide catalysts increased with time on stream and reached steady state after 3 days. This observation is contradictory with the result observed over conventional sulfide catalyst. In the case of conventional NiMo/γ-Al_2O_3 sulfide catalyst, HDN and HDS

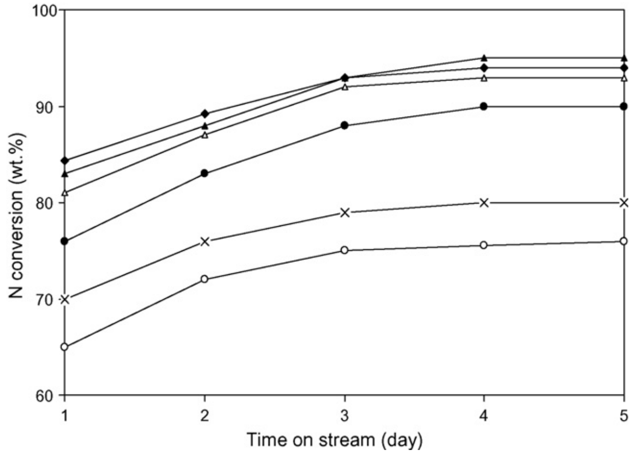

Fig. 6. The N conversion of LGO as function of time on stream during catalyst stabilization at 370 °C. (○) PNiMo(o), (×) PNiMo(0.5), (●) PNiMo(1.5), (◆) PNiMo(2.5), (△) PNiMo(3.5) and (▲) PNiMo(4.5).

activities decreased with time because of the deposition of coke on the catalyst surface and stabilized after 3–4 days [37]. The initial increase in HDN and HDS activities of these catalysts shows that there is a change in the nature of surface active sites of these catalysts during hydrotreating, and forms a new active site, which can enhance the HDN and HDS activities of carbide catalysts. The partial sulfidation of these carbide catalysts in the presence of H_2S/H_2 gas mixture at hydrotreating temperatures was evidenced by DRIFT spectroscopy of adsorbed CO. This showed that, it is possible that these carbide catalysts react with the H_2S gas produced during HDS reaction and get sulfided. As a result of sulfidation, there is a possibility that ‘‘NiMoS’’ phase could be formed on the surface of NiMo/γ-Al_2O_3 carbide catalysts. The ‘‘NiMoS’’ is the most active phase in NiMo/γ-Al_2O_3 sulfide catalyst for HDN and HDS reactions [38–40]. The ‘‘NiMoS’’ phase formed on these carbide surface are beneficial for hydrotreating of LGO and enhance the HDN and HDS activities of carbide catalysts.

3.5.2. The effect P on HDN and HDS activities of NiMo/γ-Al_2O_3 carbide catalyst

The HDN and HDS activities of the carbide catalysts after stabilization for 5 days were studied at 340, 350 and 360 °C using LGO and then at 300 °C using model feed in a trickle bed reactor. The pressure, LHSV and H_2/feed ratio were maintained at 8.8 MPa, 2 h^{-1} and 600 (v/v), and 8.8 MPa, 3 h^{-1} and 600 (v/v), respectively for LGO and model feed.

The apparent rate constant for HDN of LGO was determined by using Eq. (1) with a pseudo first order.

$$k_{\text{HDN}} = \ln\left(\frac{N_{\text{F}}}{N_{\text{P}}}\right)\text{LHSV} \tag{1}$$

where k_{HDN} is the pseudo first order HDN kinetic constant (h^{-1}); N_{F} the total nitrogen in the feedstock (wt.%); N_{P} the total nitrogen in the product (wt.%); LHSV is the liquid hourly space velocity (h^{-1}).

For HDS of LGO reaction a pseudo 1.5 order model was assumed. Thus, the corresponding apparent rate constant was calculated using the following equation:

$$k_{\text{HDS}} = \left[\frac{1}{S_{\text{P}}^{0.5}} - \frac{1}{S_{\text{F}}^{0.5}}\right]\frac{\text{LHSV}}{(n-1)} \tag{2}$$

where k_{HDS} is the pseudo 1.5 order HDS kinetic constant (wt.%$^{-0.5}$ h^{-1}); S_{P} the sulfur in product (wt.%); S_{F} the sulfur in the feedstock (wt.%); n is the order of reaction.

The HDN and HDS activities of carbide catalysts with LGO are expressed by the rate constants. Fig. 8 shows the influence of P content on the HDN rate constant at 340, 350 and 360 °C. At all temperatures studied, as the concentration of P promoter increases, the HDN activity increases to an optimum for 2.5 wt.% P. The HDN activity levels off for P contents above 2.5 wt.% of P. This is in agreement with the CO adsorption studies (Fig. 3), which also reveals maximum promotion for a P wt.% of 2.5. The increase of k_{HDN} on P addition confirmed that P acts as a promoter in NiMo/γ-Al_2O_3 carbide for HDN reaction as it does in the case of conventional NiMo/γ-Al_2O_3 sulfide catalyst.

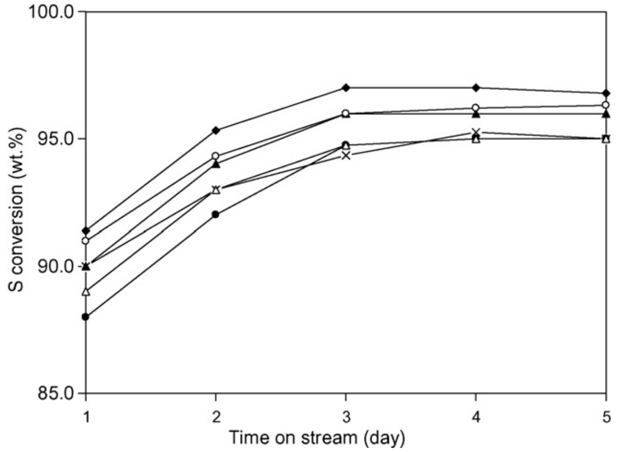

Fig. 7. The S conversion of LGO as function of time on stream during catalyst stabilization at 370 °C. (○) PNiMo(0), (×) PNiMo(0.5), (●) PNiMo(1.5), (◆) PNiMo(2.5), (△) PNiMo(3.5) and (▲) PNiMo(4.5).

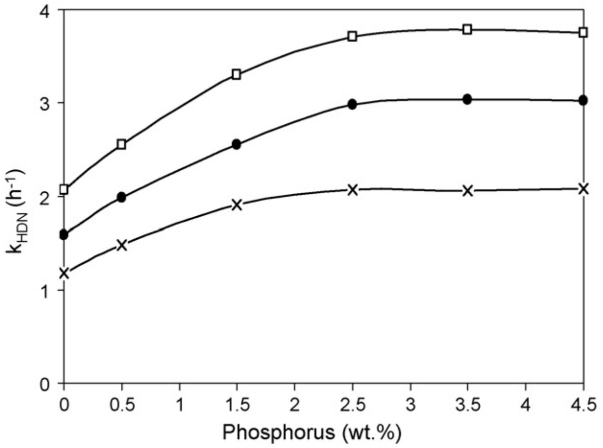

Fig. 8. The effect of P content in NiMo/γ-Al_2O_3 carbide on the HDN rate constant with LGO. (×) 340 °C, (●) 350 °C and (□) 360 °C.

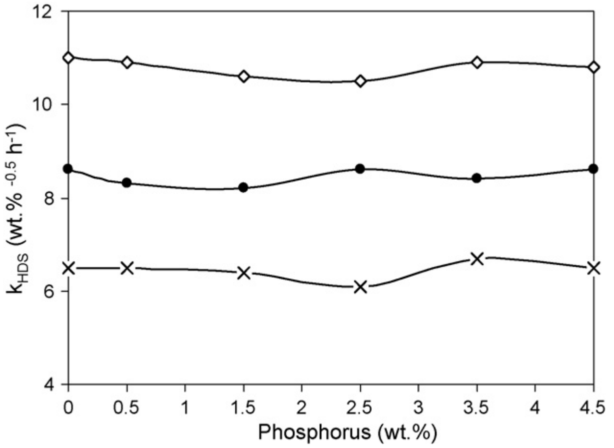

Fig. 9. The effect of P content in NiMo/γ-Al_2O_3 carbide on the HDS rate constant with LGO. (×) 340 °C, (●) 350 °C and (□) 360 °C.

Fig. 9 shows that there is no significant change in HDS rate constant of NiMo/Al_2O_3 carbide catalyst on addition of P at all temperatures studied. This indicates that the P addition to NiMo/γ-Al_2O_3 carbide does not give any synergic effect on HDS of LGO. Maity et al. [41] observed similar observation with HDS of Maya heavy crude over P promoted NiMo/γ-Al_2O_3 sulfide. P addition also led to the negative effect on NiMo/γ-Al_2O_3 sulfide in HDS of thiophene [19] and dibenzothiophene [18]. In contradiction to HDS reaction, the phosphorus addition mostly promoted the HDN activity of NiMo/γ-Al_2O_3 sulfide catalyst in industrial HDN process as well as with model compounds such as quinoline [18,19,42,43].

The HDN and HDS activities of all the carbide catalysts using model feed containing dibenzothiophene and quinoline at 300 °C are shown in Fig. 10. The HDN and HDS of model feed over molybdenum carbide catalysts follow the similar trend in N and S conversions as LGO feed with respect to P addition. P is found to be an efficient HDN promoter in the nitrogen removal from quinoline over NiMo/γ-Al_2O_3 carbide, enhanced the HDN activity and does not significantly influence the sulfur removal from dibenzothiophene. The increase in HDN activity upon P addition cannot be due to increase in dispersion of Mo_2C phase by P, since then HDN as well as HDS should have increased. So the increase in HDN conversion by P must be inherent to the mechanism of the HDN of quinoline.

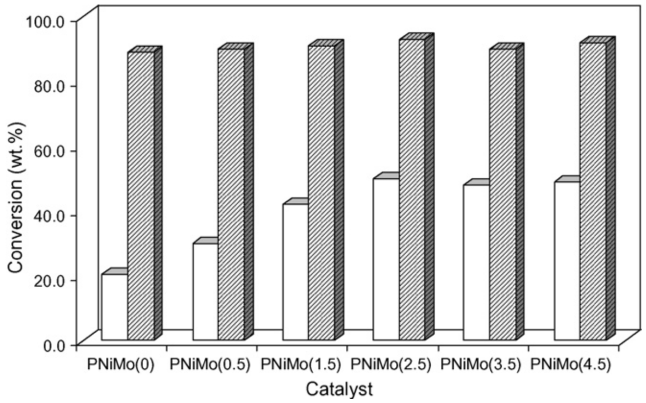

Fig. 10. The HDN and HDS of model feed over P promoted NiMo/Al_2O_3 carbide catalysts at 300 °C. (□) N conversion and (▨) S conversion.

The HDN and HDS reaction networks are complex, rather than simple single step reaction networks. In the quinoline and dibenzothiophene networks, hydrogenation as well as N- or S-removal (hydrogenolysis) reactions are present. As observed by Eijsbouts et al. [19], the effect of P in NiMo/γ-Al_2O_3 catalyst depends on whether the C–S or C–N bond breaking steps are slower or faster than the hydrogenation steps. In the HDN of quinoline C–N bond breaking is rate determining [19], and thus P addition to NiMo/γ-Al_2O_3 has a beneficial effect. In the HDS of dibenzothiophene, P has no effect. This suggests that the hydrogenation step, prior to the S removal, is rate determining over the P promoted NiMo/γ-Al_2O_3 catalysts.

The hydrogenolysis and hydrogenation (HYD) routes depend on nature of catalyst (CoMo or NiMo), H_2S partial pressure, and total pressure. The dibenzothiophene reacts mainly through the hydrogenolysis route over CoMo/Al_2O_3 catalyst [44]. But P addition to CoMo/Al_2O_3 favors the HYD route in HDS of dibenzothiophene as observed by Kwak et al. [45]. The NiMo/Al_2O_3, which is generally regarded as superior to CoMo/Al_2O_3 as hydrogenation catalysts favor the HYD route compared with CoMo/Al_2O_3 catalyst. The study by Rabarihoela-Rakotovao et al. [46] showed that hydrogenolysis route of dibenzothiophene is inhibited by the H_2S partial pressure and thus favors HYD route. Further, an increase of total pressure from 2.5 to 5.5 Mpa increased the ratio of rate of HYD to hydrogenolysis from 0.6 to 1 [46]. In the present study, the HDN and HDS reactions were carried at 8.8 MPa over P promoted NiMo/Al_2O_3 catalysts. The above reaction pressure and catalyst type may be favoring the HYD route in HDS of dibenzothiophene. Further, the higher amount of S (6500 ppm) in the feed and high conversion $\geq$90%) lead to higher H_2S partial pressure and thus favors HYD route in HDS of dibenzothiophene.

The optimum active P promoted NiMo/γ-$A1_2O_3$ carbide catalyst, PNiMo(2.5) was compared with the conventional sulfide catalyst having similar metal P, Mo and Ni loadings and also commercial P containing NiMo/γ-$A1_2O_3$ sulfide catalyst. The sulfide catalysts were found to be more active for HDN and HDS of light gas oil than the carbide catalyst on the basis of unit weight. This has been discussed in our previous publication [47].

3.6. Post reaction characterization

All the catalysts were characterized after the runs. XRD patterns of spent PNiMo(0) catalysts show presence of β-Mo_2C phase. This demonstrates that bulk structure of β-Mo_2C is preserved under hydrotreating conditions. No particles of MoS_2 are detected in spent PNiMo(0) catalyst by XRD (figure not shown). This revealed that Mo carbide is not sulfided completely under hydrotreating conditions. In the case of P promoted NiMo/γ-Al_2O_3 carbide spent catalysts, XRD patterns revealed neither Mo_2C phase nor MoS_2 phase. The characteristic peaks of the molybdenum carbides are not apparent in the above catalysts because of the fine dispersion and also the main

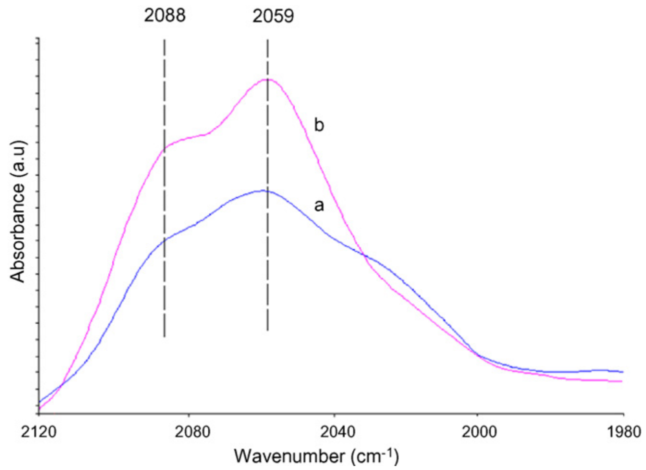

Fig. 11. DRIFT spectra of CO adsorbed on (a) spent PNiMo(0) and (b) spent PNiMo(2.5).

γ-Al_2O_3 peaks overlap within the same 2θ interval. The surface sites of selected two spent catalysts such as PNiMo(0) and PNiMo(2.5) were studied by DRIFT spectroscopy of adsorbed CO. DRIFT spectra of CO adsorption on above two spent catalysts is shown in Fig. 11. The CO adsorption patterns of the spent catalysts are different from that of corresponding fresh catalysts shown in Fig. 3. The CO adsorption bands of fresh catalysts are shifted to higher wavenumber for spent catalysts. Wu et al. [31] observed that CO adsorption band of Mo phosphides was shifted gradually to higher wavenumber with increase in sulfidation of Mo phosphides surface. Fully sulfided Mo gives CO adsorption peak around 2100 cm^{-1} [31–35]. The CO adsorption peak at 2088 cm^{-1} of spent catalysts confirmed that surface of Mo carbide catalysts are partially sulfided during the hydrotreating reaction. As a result of sulfidation, there is a possibility that ‘‘NiMoS’’ phase could be formed on the surface of carbide catalysts. Aegerter et al. [16] also observed sulfidation of Mo_2C during HDS of thiophene and proposed that a thin layer of highly dispersed MoS_2 is present on the surfaces of the Mo carbide particles. This model is further supported by McCrea et al. [17]. Further from the activity study of these carbide catalysts, it was concluded that P act as effective promoter in Mo carbide catalyst as it does in NiMo/Al_2O_3 sulfide, and promotes the HDN reaction. This revealed that active sites of these carbide catalysts during hydrotreating are similar to NiMo/Al_2O_3 sulfide catalyst.

4. Conclusions

A series of P promoted NiMo/γ-Al_2O_3 carbide catalysts with finely dispersed β-Mo_2C particles were prepared. P addition to NiMo/γ-Al_2O_3 increased the number of accessible Mo sites on the surface as a result of higher dispersion. DRIFT of adsorbed CO evidenced that NiMo/γ-Al_2O_3 carbide catalyst mostly contains Mo^{0+} species on the surface and forms Mo^{3+} species by P addition. The maximum numbers of Mo^{3+}, Mo^{2+} and Mo^{1+} surface species are found in NiMo/γ-Al_2O_3 carbide catalyst with P content of 2.5 wt.%. The change of surface sites of NiMo/γ-Al_2O_3 carbide by P addition is also evidenced by H_2-TPR of passivated carbide. All these P promoted NiMo/γ-Al_2O_3 carbide catalysts were tested in HDN and HDS of LGO and model compounds at industrial conditions. P is found to be an efficient HDN promoter for nitrogen removal from LGO and quinoline over NiMo/γ-Al_2O_3 carbide, but does not significantly influence the sulfur removal from LGO and dibenzothiophene. HDN of quinoline showed that P plays a direct role in the HDN reaction, since the removal of nitrogen from cyclic amines is rate determining step, which is promoted by P. P has no effect in the HDS of dibenzothiophene, because in the HDS of dibenzothiophene hydrogenation, preceding the S removal step is rate determining. Post reaction characterization of catalysts showed that the surface of all carbide catalysts was partially sulfided during the hydrotreating.

Acknowledgments

The authors are grateful to Syncrude Canada Ltd. and Natural Science and Engineering Research Council of Canada for financial support for this research.

References

[1] H. Abe, T.K. Cheung, A.T. Bell, Catal. Lett. 21 (1993) 11.
[2] C.C. Yu, S. Ramanathan, B. Dhandapani, J.G. Chen, S.T. Oyama, J. Phys. Chem. B 101 (1997) 512.
[3] S. Ramanathan, S.T. Oyama, J. Phys. Chem. 99 (1995) 16365.
[4] C.W. Colling, J.G. Choi, L.T. Thompson, J. Catal. 160 (1996) 35.
[5] G.M. Dolce, P.E. Savage, L.T. Thompson, Energy Fuels 11 (1997) 3.
[6] I.K. Milad, K.J. Smith, P.C. Wong, K.A.R. Mitchell, Catal. Lett. 52 (1998) 113.
[7] M. Nagai, T. Miyao, T. Tuboi, Catal. Lett. 18 (1993) 9.
[8] E.J. Markel, J.W. Van Zee, J. Catal. 126 (1990) 643.
[9] Y. Zhang, Z. Wei, W. Yan, P. Ying, C. Ji, X. Li, X. Sun, Q. Xin, Catal. Today 30 (1996) 135.
[10] P. Da Costa, C. Potvin, J.M. Manoli, J.L. Lemberton, G. Perot, G.D. Mariadassou, J. Mol. Catal. A 184 (2002) 323.
[11] J.C. Schlatter, S.T. Oyama, J.E. Metcalfe, J.M. Lambert, Ind. Eng. Chem. Res. 27 (1988) 1648.
[12] P. Da Costa, C. Potvin, J.M. Manoli, B. Genin, G.D. Mariadassou, Fuel 83 (2004) 1717.
[13] V. Schwartz, S.T. Oyama, J.G. Chen, J. Phys. Chem. B 104 (2000) 8800.
[14] B. Dhandapani, S. Ramanathan, C.C. Yu, B. Fruhberger, J.G. Chen, S.T. Oyama, J. Catal. 176 (1998) 61.
[15] D.J. Sajkowski, S.T. Oyama, Appl. Catal. A 134 (1996) 339.
[16] P.A. Aegerter, W.W.C. Quigley, G.J. Simpson, D.D. Ziegler, J.W. Logan, K.R. McCrea, S. Glazier, M.E. Bussell, J. Catal. 164 (1996) 109.
[17] K.R. McCrea, J.W. Logan, T.L. Tarbuck, J.L. Heiser, M.E. Bussell, J. Catal. 171 (1997) 255.
[18] J.A.R. van Veen, H.A. Colijn, P. Hendriks, A.J. van Welsenes, Fuel Process. Technol. 35 (1993) 137.
[19] S. Eijsbouts, J.N.M. van Gestel, J.A.R. van Veen, V.H.J. de Beer, R. Prins, J. Catal. 131 (1991) 412.
[20] S.M.A.M. Bouwens, A.M. van der Kraan, V.H.J. De Beer, R. Prins, J. Catal. 128 (1991) 559.
[21] T.C. Ho, A.J. Jacobson, R.R. Chianelli, C.R.F. Lund, J. Catal. 138 (1992) 351.
[22] R. Iwamoto, J. Grimblot, Stud. Surf. Sci. Catal. 106 (1997) 195.
[23] P. Perez-Romo, C. Potvin, J.-M. Manoli, M.M. Chehimi, G. Djega-Mariadassou, J. Catal. 208 (2002) 187.
[24] P. Da Costa, C. Potvin, J.-M. Manoli, M. Breysse, G. Djega-Mariadassou, Catal. Lett. 72 (2001) 91.

[25] L.A. Santillan-Vallejo, J.A. Melo-Banda, A.I. Reyes de la Torre, G. Sandoval-Robles, J.M. Domınguez, A. Montesinos-Castellanos, J.A. de los Reyes-Heredia, Catal. Today 109 (2005) 33.
[26] V. Sundaramurthy, A.K. Dalai, J. Adjaye, Catal. Lett. 102 (2005) 299.
[27] R. Kapoor, S.T. Oyama, B. Fruhberger, B.D. DeVries, J.G. Chen, Catal. Lett. 34 (1995) 179.
[28] S. Yang, C. Li, J. Xu, Q. Xin, J. Phys. Chem. B 102 (1998) 6986.
[29] W. Wu, Z. Wu, C. Liang, X. Chen, P. Ying, C. Li, J. Phys. Chem. B 107 (2003) 7088.
[30] W. Wu, Z. Wu, Z. Feng, P. Ying, C. Li, Phys. Chem. Chem. Phys. 6 (2004) 5596.
[31] Z. Wu, F. Sun, W. Wu, Z. Feng, C. Liang, Z. Wei, C. Li, J. Catal. 222 (2004) 41.
[32] B. Muller, A.D. Van Langeveld, J.A. Moulijn, H. Knozinger, J. Phys. Chem. 97 (1993) 9028.
[33] Z. Wu, Y. Chu, S. Yang, Z. Wei, C. Li, Q. Xin, J. Catal. 194 (2000) 23.
[34] A. Travert, C. Dujardin, F. Mauge, S. Cristol, J.F. Paul, E. Payen, D. Bougeard, Catal. Today 70 (2001) 255.
[35] Z. Wu, C. Li, Z. Wei, P. Ying, Q. Xin, J. Phys. Chem. B 106 (2002) 979.
[36] Z. Wei, Q. Xin, P. Grange, B. Delmon, J. Catal. 168 (1997) 176.
[37] D. Ferdous, A.K. Dalai, J. Adjaye, Fuel 85 (2006) 1286.
[38] N.-Y. Topsøe, H. Topsøe, O. Sørensen, B.S. Clausen, R. Candia, Bull. Soc. Chim. Belg. 93 (1984) 727.
[39] N.Y. Topsoe, H. Topsoe, J. Catal. 84 (1983) 386.
[40] S.P.A. Louwers, R. Prins, J. Catal. 139 (1993) 525.
[41] S.K. Maity, J. Ancheyta, L. Soberanis, F. Alonso, Appl. Catal. A 250 (2003) 231.
[42] A.L. Morales, R.E. Galiasso, M.M. Agudelo, J.A. Salazar, A.L. Carrasquel, U.S. Patent 4,520,128 (1985).
[43] R.E. Tischer, N.K. Narain, G. Stiegel, D. Cillo, Ind. Eng. Chem. Res. 26 (1987) 422.
[44] B.C. Gates, H. Topsøe, Polyhedron 16 (1997) 3213.
[45] C. Kwak, M.Y. Kim, K. Choi, S.H. Moon, Appl. Catal. A 185 (1999) 19.
[46] V. Rabarihoela-Rakotovao, S. Brunet, G. Perot, F. Diehl, Appl. Catal. A 306 (2006) 34.
[47] V. Sundaramurthy, A.K. Dalai, J. Adjaye, Appl. Catal. A 311 (2006) 155.